

On the Efficiency of 5(4) RK-Embedded Pairs with High Order Compact Scheme and Robin Boundary Condition for Options Valuation

Chinonso Nwankwo^{a,*}, Weizhong Dai^b

^a Modelling and Simulation, CEMSE, KAUST, Thuwal, Saudi Arabia

^b Department of Mathematics and Statistics, Louisiana Tech University, Ruston LA 71272, USA

* Corresponding author, nonsonwankwo@gmail.com, <https://orcid.org/0000-0001-5526-1337>

Abstract

When solving the American options with or without dividends, numerical methods often obtain lower convergence rates if further treatment is not implemented even using high-order schemes. In this article, we present a fast and explicit fourth-order compact scheme for solving the free boundary options. In particular, the early exercise features with the asset option and option sensitivity are computed based on a coupled of nonlinear PDEs with fixed boundaries for which a high order analytical approximation is obtained. Furthermore, we implement a new treatment at the left boundary by introducing a third-order Robin boundary condition. Rather than computing the optimal exercise boundary from the analytical approximation, we simply obtain it from the asset option based on the linear relationship at the left boundary. As such, a high order convergence rate can be achieved. We validate by examples that the improvement at the left boundary yields a fourth-order convergence rate without further implementation of mesh refinement, Rannacher time-stepping, and/or smoothing of the initial condition. Furthermore, we extensively compare, the performance of our present method with several 5(4) Runge-Kutta pairs and observe that Dormand and Prince and Bogacki and Shampine 5(4) pairs are faster and provide more accurate numerical solutions. Based on numerical results and comparison with other existing methods, we can validate that the present method is very fast and provides more accurate solutions with very coarse grids.

Keywords: Dividend and non-dividend options, high order analytical approximation, optimal exercise boundary, compact scheme, Robin boundary condition, Runge-Kutta- 5(4) pairs

1. Introduction

Suppose $P(S, \tau)$ and $f_b(\tau)$ and E are the put option price, optimal exercise boundary, and strike price, respectively, and $\tau = T - t$. Then, $P(S, \tau)$ satisfies the free boundary value problem:

$$\frac{\partial P(S, \tau)}{\partial \tau} - \frac{1}{2} \sigma^2 S^2 \frac{\partial^2 P(S, \tau)}{\partial S^2} - (\mu - \delta) S \frac{\partial P(S, \tau)}{\partial S} + (\mu - \rho) P(S, \tau) = \zeta, \quad S > f_b(\tau); \quad (1a)$$

$$P(S, \tau) = E - S, \quad S < f_b(\tau). \quad (1b)$$

Here, ζ and ρ are values that could represent models which include the jump-diffusion model, regime-switching model, one-dimensional FX options, or American options. If $\mu \in [r, r_d]$, $\delta \in [r_f, D, 0]$, $\zeta = 0$, and $\rho = 0$, we have a model suitable for solving American and FX options. In this case, r_d and r_f are the domestic and foreign interest rates, respectively, for one-dimensional FX options. r and D are the interest rate and the dividend, respectively, for non-dividend and dividend American options. If we consider the latter, (1) reduces to

$$\frac{\partial P(S, \tau)}{\partial \tau} - \frac{1}{2} \sigma^2 S^2 \frac{\partial^2 P(S, \tau)}{\partial S^2} - (r - D) S \frac{\partial P(S, \tau)}{\partial S} + r P(S, \tau) = 0, \quad S > f_b(\tau); \quad (2a)$$

$$P(S, \tau) = E - S, \quad S < f_b(\tau). \quad (2b)$$

The initial and boundary conditions are given as

$$P(S, 0) = \max(E - S, 0), \quad f_b(0) = E; \quad (2c)$$

$$P(f_b, \tau) = E - f_b(\tau), \quad P(0, \tau) = E, \quad P(\infty, \tau) = 0, \quad \frac{\partial}{\partial S} P(f_b, \tau) = -1. \quad (2d)$$

After the first algorithm for solving the American option pricing model was proposed by Brennan and Schwartz (1977), other several methods have further been introduced. For the American options with or without dividends, mostly, the first-order and second-order explicit and implicit schemes have been implemented (Company et al., 2014; Company et al., 2016; Holmes and Yang, 2008; Nielsen et al., 2002; Song et al., 2017; Zhang et al., 2014, Wu and Kwok, 1997). This is because the first and second-order convergence rates can easily be obtained using these schemes. Few authors have proposed high-order numerical methods for solving American style options with or without dividends (Ballestra, 2018; Cen and Chen, 2019; Christara and Dang, 2011; Hajipour and Malek, 2015; Tangman et al., 2008; Zhao et al., 2007). Some of these authors that implemented high order numerical scheme either did not provide the result of the convergence rate or obtained a numerical convergence rate that is either not in good agreement with the theoretical convergence rate (Hajipour and Malek, 2015; Tangman et al., 2008; Zhao et al., 2007) or unstable. For instance, even with an efficient fourth-order compact scheme, only the second-order convergence rate should be expected. Certain improvements have been proposed for recovering high order convergence rate which includes grid refinement and stretching (Osterlee et al., 2005) smoothing of the initial condition (Forsyth and Vetzal, 2002; Pooley et al., 2003; Christara et al., 2011), repeated

Richardson extrapolation (Ballestra, 2018), etc. Some of these improvements either are difficult to implement or require an additional computational cost. This increases the overall computational burden for approximating American-style options.

Here, to reduce computational cost substantially and recover the fourth-order convergence rate with a fourth-order compact scheme, we first implement a special treatment from the information on the left boundary. We then propose a simple, efficient, and fast fourth-order compact scheme with Robin boundary condition and RK-embedded 5(4) pairs for approximating (2). It is well known that in the location of large variation and sufficient smoothness, smaller and larger time steps, respectively, might be required to achieve more accurate numerical approximations. Several embedded Runge-Kutta pairs have been developed and implemented to address this issue in the literature (Bogacki, 1996; Bogacki and Shampine, 1996; Cash and Karp, 1990; Dormand and Prince, 1980; Fehlberg, 1969; Hoover et al., 2016; Ketcheson et al., 2020; Macdougall and Verner, 2002; Papakostas and Papageorgiou, 1996; Simos, 1993; Simos and Papakaliatakis, 1998; Simos and Tsitouras, 2018; Tsitouras, 1998; Wilkie and Cetinbas, 2005; William and Saul, 1992). It is worth noting that the performance of some of these embedded pairs is model-dependent. Even though most of the option pricing models exhibit some form of discontinuity and variation, however, these embedded pairs have not attracted much attention in options valuation. It is in our interest to investigate the performance of our present method with several 5(4) RK-embedded pairs and validate the ones more suitable for solving dividend-paying American options.

The rest of the paper is organized as follows. In section 2, we present a semi-analytical approach for computing the time-dependent coefficient that introduces the nonlinearity in the transformed model. In section 3, we present the high-order numerical scheme for the approximation of the optimal exercise boundary simultaneously with the asset option and option sensitivity. In section 4, we discuss our numerical experiment and compare the performance of our proposed method with several 5(4) RK-embedded pairs. Furthermore, we compare our numerical results with the well-known existing methods and conclude the paper in section 5.

2. Semi-Analytical Formulation with Time-Dependent Coefficient

Considering the free boundary problem for pricing options, the early exercise feature needs to be computed simultaneously with the options. To achieve this possibility, we first fix the free boundary by introducing the transformed relationship (Company et al., 2016; Egorova et al., 2016; Wu and Kwok, 1997) below to (2)

$$x = \ln S - \ln s_f(\tau), \quad U(x, \tau) = P(S, \tau). \quad (3)$$

With this transformation, we obtained a coupled nonlinear PDE equation for the asset option as follows:

$$U_\tau(S, \tau) - \frac{1}{2}\sigma^2 U_{xx}(S, \tau) - \omega(\tau)V(S, \tau) + rU(S, \tau) = 0, \quad x > 0; \quad (4a)$$

$$U(x, \tau) = K - S = K - s_f(\tau)e^x, \quad x < 0. \quad (4b)$$

Taking the derivative of (4a) with respect to x and denoting $V = U_x$, we obtain a coupled nonlinear PDE equation for delta option as follows:

$$V_\tau(S, \tau) - \frac{1}{2}\sigma^2 V_{xx}(S, \tau) - \omega(\tau)\frac{1}{2}\sigma^2 U_{xx} + rV(S, \tau) = 0, \quad x > 0; \quad (4c)$$

$$V(x, \tau) = -S = -s_f(\tau)e^x, \quad x < 0. \quad (4d)$$

The initial and boundary conditions for the asset option and option sensitivity are given as follows:

$$U(x, 0) = \max(K - Ke^x, 0) = 0, \quad x \geq 0, \quad s_f(0) = K; \quad (4e)$$

$$U(0, \tau) = K - s_f(\tau), \quad U(\infty, \tau) = 0, \quad (4f)$$

$$V(0, \tau) = -s_f(\tau), \quad V(\infty, \tau) = 0. \quad (4g)$$

The non-linearity in the transformed coupled system of PDEs is due to the coefficient of the convective term

$$\omega(\tau) = (r - D) + \frac{f'_b(\tau)}{f_b(\tau)} - \frac{\sigma^2}{2}, \quad (5)$$

which is time-dependent and involves the derivative of the optimal exercise boundary. By implementing a front-fixing approach, we focus on the space domain $[0, \infty)$ with the fixed boundary representing the left boundary point. It is important to mention that with this approach, the non-smoothness in the second derivative of the asset option is no longer visible [see the work of Ballestra (2018)]. However, another source of non-smoothness arises due to the time-dependent coefficient in (5). This is because $f_b(\tau)$ is not differentiable when $\tau = 0$ [see Ballestra (2018), Chen and Chadam (2007), Mallier (2002)]. Chen and Chadam (2007) explained that the non-differentiability of $f_b(\tau)$ when $\tau = 0$ is due to the non-smoothness of the maximum function at the payoff. Ballestra (2018) further mentioned that if the source of this non-smoothness is efficiently handled, then a high order convergent rate can be expected with the front-fixing approach.

To handle this source of non-smoothness, Ballestra (2018) implemented a time variable transformation. Here, we derive a high order analytical formulation for obtaining a precise approximation of (5) without time discretization and then approximate (3) with high order compact finite difference scheme. To this end, we first introduce a transformation with intermediate function (that has Lipschitz character near the left boundary) as follows (Kim et al., 2013; Kim et al., 2017):

$$L(x, \tau) = \sqrt{U(x, \tau) - E + e^x f_b(\tau)}, \quad (6a)$$

with

$$L(x, \tau) \begin{cases} = 0, & x \in [\ln s_f(\infty) - \ln s_f(0)], \\ > 0, & x \in (0, \infty). \end{cases} \quad (6b)$$

Here, we consider the derivative of the intermediate function up to the third-order derivative as follows:

$$U(x, \tau) = L^2(x, \tau) + E - e^x f_b(\tau), \quad U(0, \tau) = E - f_b(\tau), \quad (7a)$$

$$U_x = 2LL' - e^x f_b(\tau), \quad U_x(0, \tau) = -f_b(\tau). \quad (7b)$$

Following the work of Goodman and Ostrov (2002), we differentiate $U(x, \tau)$ with respect to τ when $x = 0$ as follows:

$$U_x \ln 1 + U_\tau = -f_b'(\tau), \quad U_\tau = -f_b'(\tau). \quad (7c)$$

Furthermore,

$$U_{xx} = 2(L')^2 + 2LL'' - e^x f_b(\tau), \quad U_{xx}(0, \tau) = 2(L'(0, \tau))^2 - f_b(\tau). \quad (7d)$$

Substituting (6) in (3a), we obtain

$$L'(0, \tau) = \frac{\sqrt{rE - Df_b(\tau)}}{\sigma}. \quad (7e)$$

The analysis of (7e) is similar to the one presented in the work of Kim et al. (2013). We would further love to point out that when $D \neq 0$, $r \geq Df_b(\tau)/E$ is required to ensure a real value of $L'(0, \tau)$. Hence at the payoff when $f_b(0) = E$, $r \geq D$ will ensure a real value of $L'(0, \tau)$. If $D = 0$, such a condition will not be imposed.

Next, we compute the derivative of $U(x, \tau)$ in (3b) as follows:

$$U_{xxx} = 6L'L'' + 2LL''' - e^x f_b(\tau), \quad U_{xxx}(0, \tau) = 6L'L'' - f_b(\tau); \quad (8a)$$

$$U_{xx} \ln 1 + U_{x\tau} = -f_b'(\tau), \quad U_{x\tau}(0, \tau) = -f_b'(\tau). \quad (8b)$$

Substituting (8) in (3b), we obtain

$$L''(0, \tau) = -\frac{2L'(0, \tau)}{3\sigma^2} \xi_\tau - \frac{2L'(0, \tau)}{3\sigma^2} \kappa - \frac{Df_b(\tau)}{3\sigma^2 L'(0, \tau)}. \quad (9)$$

Here, $\xi_\tau = f'_b(\tau)/f_b(\tau)$ and $\kappa = r - D - \sigma^2/2$. Finally, we further take the derivative of (3b) with respect to x and obtain:

$$U_{xxt}(S, \tau) - \frac{1}{2}\sigma^2 U_{xxxx}(S, \tau) - \omega(\tau)U_{xxx} + rU_{xx} = 0. \quad (10)$$

Computing the partial derivatives in (8), we obtain as follows:

$$U_{xxxx} = 6(L'')^2 + 8L'L''' - e^x f_b(\tau), \quad U_{xxxx}(0, \tau) = 2(L')^2 - f_b(\tau); \quad (11a)$$

$$U_{xxx} \ln 1 + U_{xxt} = -\frac{2Df'_b(\tau)}{\sigma^2} - f'_b(\tau), \quad U_{xxt}(0, \tau) = -\frac{2Df'_b(\tau)}{\sigma^2} - f'_b(\tau). \quad (11b)$$

Substituting (9) in (8), we obtain

$$L'''(0, \tau) = \frac{2L'(0, \tau)}{3\sigma^4} \xi_\tau^2 + \left[\frac{4L'(0, \tau)\kappa}{3\sigma^4} - \frac{2Df_b(\tau)}{3\sigma^2 L'(0, \tau)} \right] \xi_\tau + \frac{2L'(0, \tau)\kappa^2}{3\sigma^4} + \frac{Df_b(\tau)\kappa}{6\sigma^4 L'(0, \tau)} - \frac{(Df_b(\tau))^2}{12\sigma^4 [L'(0, \tau)]^3} + \frac{rL'(0, \tau)}{2\sigma^2} - \frac{Df_b(\tau)}{4\sigma^2 L'(0, \tau)}. \quad (12)$$

It is worth mentioning that ξ_τ is involved in the interior discretization of the system of PDEs. Moreover, we intend to discretize in space using a fourth-order compact finite difference scheme. Hence, we need to derive the analytical approximation of ξ_τ up to the fourth-order accuracy in space. To this end, we introduce an extrapolated Taylor series expansion of $L(\tilde{x}, \tau)$ at $x = 0$ up to the seventh order accuracy as follows:

$$\begin{aligned} \alpha_0 L(0, \tau) + \alpha_1 L(\tilde{x}, \tau) + \alpha_2 L(2\tilde{x}, \tau) + \alpha_3 L(3\tilde{x}, \tau) + \alpha_4 L(4\tilde{x}, \tau) \\ = \gamma_0 \tilde{x} L'(0, \tau) + \gamma_1 \tilde{x}^2 L''(0, \tau) + \gamma_2 \tilde{x}^3 L'''(0, \tau) + O(\tilde{x}^{n+3}). \end{aligned} \quad (13a)$$

Here,

$$\alpha_0 = \frac{3445}{27}, \quad \alpha_1 = 256, \quad \alpha_2 = -48, \quad \alpha_3 = \frac{256}{27}, \quad \alpha_4 = -1; \quad (13b)$$

$$\gamma_0 = \frac{4980}{27}, \quad \gamma_1 = \frac{600}{9}, \quad \gamma_2 = \frac{32}{3}. \quad (13c)$$

With Taylor series expansion and method of extrapolation, it is straightforward to obtain the coefficients in (13b) and (13c). Hence, for brevity, we skip its detailed derivation. Here, $\tilde{x} \ll x$. Substituting (7), (9), and (12) into (13a), we obtain a high order analytical approximation of ξ_τ in quadratic form as follows:

$$g_2(\xi_\tau)^2 + g_1\xi_\tau + g_0 = 0, \quad \omega(\tau) = \xi_\tau + \kappa. \quad (14a)$$

Here,

$$g_2 = \frac{2L'(0, \tau)\gamma_2\tilde{x}^3}{3\sigma^4}, \quad (14b)$$

$$g_1 = \left[\frac{4L'(0, \tau)\kappa}{3\sigma^4} - \frac{2Df_b(\tau)}{3\sigma^2L'(0, \tau)} \right] \gamma_2\tilde{x}^3 - \frac{2L'(0, \tau)\gamma_1\tilde{x}^2}{3\sigma^2}, \quad (14c)$$

$$g_{0,4} = \left[\frac{2L'(0, \tau)\kappa^2}{3\sigma^4} + \frac{Df_b(\tau)\kappa}{6\sigma^4L'(0, \tau)} - \frac{(Df_b(\tau))^2}{12\sigma^4[L'(0, \tau)]^3} + \frac{rL'(0, \tau)}{2\sigma^2} - \frac{Df_b(\tau)}{4\sigma^2L'(0, \tau)} \right] \gamma_2\tilde{x}^3 \\ - \left[\frac{2L'(0, \tau)}{3\sigma^2}\kappa + \frac{Df_b(\tau)}{3\sigma^2L'(0, \tau)} \right] \gamma_1\tilde{x}^2 + \gamma_0\tilde{x}L'(0, \tau) - M_4(\tilde{x}, \tau), \quad (14d)$$

$$M_4(\tilde{x}, \tau) = \alpha_1L(\tilde{x}, \tau) + \alpha_2L(2\tilde{x}, \tau) + \alpha_3L(3\tilde{x}, \tau) + \alpha_4L(4\tilde{x}, \tau). \quad (14e)$$

3. Numerical Discretization

To construct our numerical scheme, we first define our computational domain. Because the asset and delta option options vanish rapidly as the value of x increases, the infinite space domain $[0, \infty) \times [0, T]$ is replaced with a bounded domain $[0, x_M] \times [0, T]$ and the right boundary is given as

$$U(x_M, \tau) = V(x_M, \tau) = 0. \quad (15)$$

Furthermore, we consider a uniform grid size as follows:

$$x_i = ih, \quad h = \frac{x_M}{M}, \quad i \in [0, M], \quad (16)$$

M and N represent the total number of grid points and time steps, respectively. The solutions of the asset option, Greeks, and the optimal exercise boundary for each regime are given as u_i^n, v_i^n , and f_b^n , respectively.

3.1. Numerical Schemes

In our present method, the optimal exercise boundary is computed from the asset option based on their linear relationship as follows:

$$U(0, \tau) = E - f_b(\tau). \quad (17)$$

To this end, we introduce a boundary condition for computing the asset option when $x = 0$ by considering the following lemma.

Lemma. Assume $f(x) \in C^5[x_0, x_1]$, then it holds

$$\frac{7}{24}f'''(x_0) + \frac{6}{24}f'''(x_1) - \frac{1}{24}f'''(x_2) = \frac{1}{h^2}[f(x_1) - f(x_0)] - \frac{1}{h}f'(x_0) + O(h^3). \quad (18)$$

Proof. For (18a), we first introduce a well-known third-order boundary condition (Yan et al., 2019) as follows:

$$\frac{10}{24}f'''(x_0) + \frac{2}{24}f'''(x_1) = \frac{1}{h^2}[f(x_1) - f(x_0)] - \frac{1}{h}f'(x_0) - \frac{h}{12}f^{(3)}(x_0) + O(h^3). \quad (19a)$$

Next, we approximate the third-order derivative as follows:

$$\frac{h}{12}f'''(x_0) = -\frac{1}{8}f'''(x_0) + \frac{1}{6}f'''(x_1) - \frac{1}{24}f'''(x_2) + O(h^3). \quad (19b)$$

Substituting (19b) into (19a), we then complete the proof for (18). For the interior nodes, we consider a fourth-order compact finite difference scheme as follows:

$$f''(x_{i-1}) + 10f''(x_i) + f''(x_{i+1}) = \frac{12}{h^2}[f(x_{i-1}) - 2f(x_i) + f(x_{i+1})] + O(h^4). \quad (20)$$

By introducing a Robin boundary condition based on the relationship between the asset option, option sensitivity, and optimal exercise boundary as follows:

$$V(0, \tau) - U(0, \tau) = -K, \quad (21a)$$

where $V = U_x$, the matrix-vector form for the asset option is as follows:

$$A = \frac{24}{h^2} \begin{bmatrix} -a & 1 & 0 & \cdots & & & & & & 0 \\ 1 & -2 & 1 & & & & & & & \vdots \\ & & 1 & -2 & 1 & & & & & \\ & & & 1 & -2 & 1 & & & & \\ 0 & & & & \ddots & \ddots & \ddots & & & 0 \\ \vdots & & & & & & 1 & -2 & 1 & \\ 0 & & & & & & & 1 & -2 & 1 \\ & & & & & & \cdots & 0 & 1 & -2 \end{bmatrix}_{M \times M},$$

$$B = \begin{bmatrix} 7 & 6 & -1 & 0 & 0 & \cdots & 0 \\ 1 & 10 & 1 & & & & \vdots \\ & & 1 & 10 & 1 & & \\ & & & 1 & 10 & 1 & \\ 0 & & & & \ddots & \ddots & \ddots & 0 \\ \vdots & & & & & & 1 & 10 & 1 \\ 0 & \cdots & 0 & 0 & 0 & 0 & 10 & 1 \end{bmatrix}_{M \times M}, \quad f_u = \frac{24}{h^2} \begin{bmatrix} K \\ 0 \\ 0 \\ \vdots \\ 0 \\ 0 \end{bmatrix}_{M \times 1}; \quad (21b)$$

$$\mathbf{u}'' = B^{-1}(A\mathbf{u}^n + \mathbf{f}_u^n), \quad (21c)$$

$$\frac{\partial \mathbf{u}}{\partial \tau} = \mathbf{v}(\mathbf{u}, \mathbf{v}) = \frac{\sigma^2}{2} B^{-1}(A\mathbf{u}^n + \mathbf{f}_u^n) + \omega(\tau)\mathbf{v} - r\mathbf{u}. \quad (21d)$$

Here, $a = 1 + h > 1$. It is worth mentioning that the third-order Robin boundary preserves diagonal dominance in both matrices. The boundary-value of the delta option can easily be computed from the optimal exercise boundary as follows:

$$V(0, \tau) = -f_b(\tau). \quad (22)$$

For the delta option, we discretize the interior nodes with (20). For $i = 1$ and $i = M - 1$, we employ a discretization as follows (Zhao, 2007; Bhatt and Khaliq, 2016):

$$14f''(x_1) - 5f''(x_2) + 4f''(x_3) - f''(x_4) = \frac{12}{h^2} [f(x_0) - 2f(x_1) + f(x_2)] + O(h^4), \quad (23a)$$

$$\begin{aligned} 14f''(x_{M-1}) - 5f''(x_{M-2}) + 4f''(x_{M-3}) - f''(x_{M-4}) \\ = \frac{12}{h^2} [f(x_{M-2}) - 2f(x_{M-1}) + f(x_M)] + O(h^4). \end{aligned} \quad (23b)$$

The matrix-vector form for the delta option is as follows:

$$F = \frac{12}{h^2} \begin{bmatrix} -2 & 1 & 0 & \dots & & & & & & & 0 \\ 1 & -2 & 1 & & & & & & & & \vdots \\ & & 1 & -2 & 1 & & & & & & \\ & & & 1 & -2 & 1 & & & & & 0 \\ 0 & & & & \ddots & \ddots & \ddots & & & & \\ \vdots & & & & & & 1 & -2 & 1 & & \\ 0 & & & & & & & 1 & -2 & 1 & \\ & & & & & & \dots & 0 & 1 & -2 & \end{bmatrix}_{M-1 \times M-1},$$

$$G = \begin{bmatrix} 14 & -5 & 4 & -1 & 0 & \dots & 0 \\ 1 & 10 & 1 & & & & \vdots \\ & & 1 & 10 & 1 & & \\ & & & 1 & 10 & 1 & \\ 0 & & & \ddots & \ddots & \ddots & 0 \\ \vdots & & & & & & 1 & 10 & 1 \\ 0 & \dots & 0 & -1 & 4 & -5 & 14 \end{bmatrix}_{M-1 \times M-1},$$

$$\mathbf{f}_v = \frac{12}{h^2} \begin{bmatrix} v_0 \\ 0 \\ 0 \\ \vdots \\ 0 \\ v_M = 0 \end{bmatrix}_{M-1 \times 1}; \quad (24a)$$

$$\mathbf{v}'' = G^{-1}(F\mathbf{v} + \mathbf{f}_v), \quad (24b)$$

$$\frac{\partial \mathbf{v}}{\partial \tau} = \mathbf{v}(\mathbf{u}, \mathbf{v}) = \frac{\sigma^2}{2} G^{-1}(F\mathbf{v} + \mathbf{f}_v) + \omega(\tau)G^{-1}(F\mathbf{u} + \mathbf{f}_u) - r\mathbf{v}. \quad (24c)$$

For the time integration, we compare the performance and accuracy of several 5(4) embedded Runge-Kutta methods. Specifically, we consider Dormand and Prince 5(4) (Dormand and Prince, 1980), Cash and

Karp 5(4), (Cash and Karp, 1990), Bogacki and Shampine 5(4) (Bogacki and Shampine, 1996), Simos and Tsitouras 5(4) (Simos and Tsitouras, 2018), and Papakostas and Papageorgiou 5(4) (Papakostas and Papageorgiou, 1996) embedded pairs. We only describe the effective implementation of Dormand and Prince 5(4) and refer the readers to the work of (Bogacki and Shampine, 1996; Cash and Karp, 1990; Simos and Tsitouras, 2018; Papakostas and Papageorgiou, 1996; Ketcheson et al., 2020) on how to obtain the coefficient entries of the other Runge-Kutta pairs which we considered in this work. To this end, we first present the semi-discretized coupled nonlinear equations in (21) and (24) as follows:

$$\frac{\partial \mathbf{u}^n}{\partial \tau} = \mathbf{v}^n = \frac{\sigma^2}{2} B^{-1} (A \mathbf{u}^n + \mathbf{f}_u^n) + \omega^n(\tau) \mathbf{v}^n - r \mathbf{u}^n, \quad (25a)$$

$$\frac{\partial \mathbf{v}^n}{\partial \tau} = \mathbf{v}^n = \frac{\sigma^2}{2} G^{-1} (G \mathbf{v}^n + \mathbf{f}_v^n) + \omega^n(\tau) G^{-1} (F \mathbf{u}^n + \mathbf{f}_u^n) - r \mathbf{v}^n. \quad (25b)$$

The error for the embedded pairs is estimated as

$$e_u = \|\tilde{\mathbf{u}}^{n+1} - \mathbf{u}^{n+1}\|_\infty, \quad e_v = \|\tilde{\mathbf{v}}^{n+1} - \mathbf{v}^{n+1}\|_\infty. \quad (25c)$$

Here, \mathbf{u}^{n+1} and \mathbf{v}^{n+1} are the numerical approximations of the asset option and option sensitivity with the fifth-order accuracy in time and the fourth-order accuracy in space, respectively. We would love to point out that we consider both the error estimate of the asset option and option sensitivity in this work. $\tilde{\mathbf{u}}^{n+1}$, \mathbf{u}^{n+1} , \mathbf{f}_b^{n+1} , $\tilde{\mathbf{v}}^{n+1}$, and \mathbf{v}^{n+1} are computed simultaneously with Dormand and Prince 5(4) coefficients as follows:

$$\mathbf{u}^{n(1)} = \mathbf{u}^n, \quad \mathbf{v}^{n(1)} = \mathbf{v}^n, \quad \mathbf{f}_b^{n(1)} = \mathbf{f}_b^n; \quad (26a)$$

$$\xi_{n(1)} = \frac{-g_1 - \sqrt{g_1^2 - 4g_2g_{0,4,n(1)}}}{2g_2}, \quad \omega^{n(1)} = \xi_{n(1)} + \kappa; \quad (26b)$$

$$\mathbf{R}_u^1 = \nu(\mathbf{u}^{n(1)}, \mathbf{v}^{n(1)})k, \quad \mathbf{R}_v^1 = \nu(\mathbf{u}^{n(1)}, \mathbf{v}^{n(1)})k; \quad (26c)$$

$$\mathbf{u}^{n(2)} = \mathbf{u}^n + \frac{k}{5} \mathbf{R}_u^1, \quad \mathbf{f}_b^{n(2)} = K - \mathbf{u}_1^{n(2)}, \quad \mathbf{v}_1^{n(2)} = -\mathbf{f}_b^{n(2)}, \quad \mathbf{v}^{n(2)} = \mathbf{v}^n + \frac{k}{5} \mathbf{R}_v^1; \quad (26d)$$

$$\xi_{n(2)} = \frac{-g_1 - \sqrt{g_1^2 - 4g_2g_{0,4,n(2)}}}{2g_2}, \quad \omega^{n(2)} = \xi_{n(2)} + \kappa; \quad (26e)$$

$$\mathbf{R}_u^2 = \nu(\mathbf{u}^{n(2)}, \mathbf{v}^{n(2)})k, \quad \mathbf{R}_v^2 = \nu(\mathbf{u}^{n(2)}, \mathbf{v}^{n(2)})k; \quad (26f)$$

$$\mathbf{u}^{n(3)} = \mathbf{u}^n + \frac{3k}{40} \mathbf{R}_u^1 + \frac{9k}{40} \mathbf{R}_u^2, \quad \mathbf{f}_b^{n(3)} = K - \mathbf{u}_1^{n(3)}; \quad (26g)$$

$$\mathbf{v}_1^{n(3)} = -f_b^{n(3)}, \quad \mathbf{v}^{n(3)} = \mathbf{v}^n + \frac{3k}{40} \mathbf{R}_v^1 + \frac{9k}{40} \mathbf{R}_v^2; \quad (26h)$$

$$\xi_{n(3)} = \frac{-g_1 - \sqrt{g_1^2 - 4g_2g_{0,4,n(3)}}}{2g_2}, \quad \omega^{n(3)} = \xi_{n(3)} + \kappa; \quad (26i)$$

$$\mathbf{R}_u^3 = v(\mathbf{u}^{n(3)}, \mathbf{v}^{n(3)})k, \quad \mathbf{R}_v^3 = v(\mathbf{u}^{n(3)}, \mathbf{v}^{n(3)})k; \quad (26j)$$

$$\mathbf{u}^{n(4)} = \mathbf{u}^n + \frac{44k}{45} \mathbf{R}_u^1 - \frac{56k}{15} \mathbf{R}_u^2 + \frac{32k}{9} \mathbf{R}_u^3, \quad f_b^{n(4)} = K - \mathbf{u}_1^{n(4)}; \quad (26k)$$

$$\mathbf{v}_1^{n(4)} = -f_b^{n(4)}, \quad \mathbf{v}^{n(4)} = \mathbf{v}^n + \frac{44k}{45} \mathbf{R}_v^1 - \frac{56k}{15} \mathbf{R}_v^2 + \frac{32k}{9} \mathbf{R}_v^3; \quad (26l)$$

$$\xi_{n(4)} = \frac{-g_1 - \sqrt{g_1^2 - 4g_2g_{0,4,n(4)}}}{2g_2}, \quad \omega^{n(4)} = \xi_{n(4)} + \kappa; \quad (26m)$$

$$\mathbf{R}_u^4 = v(\mathbf{u}^{n(4)}, \mathbf{v}^{n(4)})k, \quad \mathbf{R}_v^4 = v(\mathbf{u}^{n(4)}, \mathbf{v}^{n(4)})k; \quad (26n)$$

$$\mathbf{u}^{n(5)} = \mathbf{u}^n + \frac{19732k}{6561} \mathbf{R}_u^1 - \frac{25360k}{2187} \mathbf{R}_u^2 + \frac{64448k}{6561} \mathbf{R}_u^3 - \frac{212k}{729} \mathbf{R}_u^4, \quad f_b^{n(5)} = K - \mathbf{u}_1^{n(5)}; \quad (26o)$$

$$\mathbf{v}_1^{n(5)} = -f_b^{n(5)}, \quad \mathbf{v}^{n(5)} = \mathbf{v}^n + \frac{19732k}{6561} \mathbf{R}_v^1 - \frac{25360k}{2187} \mathbf{R}_v^2 + \frac{64448k}{6561} \mathbf{R}_v^3 - \frac{212k}{729} \mathbf{R}_v^4; \quad (26p)$$

$$\xi_{n(5)} = \frac{-g_1 - \sqrt{g_1^2 - 4g_2g_{0,4,n(5)}}}{2g_2}, \quad \omega^{n(5)} = \xi_{n(5)} + \kappa; \quad (26q)$$

$$\mathbf{R}_u^5 = v(\mathbf{u}^{n(5)}, \mathbf{v}^{n(5)})k, \quad \mathbf{R}_v^5 = v(\mathbf{u}^{n(5)}, \mathbf{v}^{n(5)})k; \quad (26r)$$

$$\mathbf{u}^{n(6)} = \mathbf{u}^n + \frac{9017k}{3168} \mathbf{R}_u^1 - \frac{355k}{33} \mathbf{R}_u^2 + \frac{46732k}{5247} \mathbf{R}_u^3 + \frac{49k}{176} \mathbf{R}_u^4 - \frac{5103k}{18656} \mathbf{R}_u^5, \quad f_b^{n(6)} = K - \mathbf{u}_1^{n(6)}; \quad (26s)$$

$$\mathbf{v}_1^{n(6)} = -f_b^{n(6)}, \quad \mathbf{v}^{n(6)} = \mathbf{v}^n + \frac{9017k}{3168} \mathbf{R}_v^1 - \frac{355k}{33} \mathbf{R}_v^2 + \frac{46732k}{5247} \mathbf{R}_v^3 + \frac{49k}{176} \mathbf{R}_v^4 - \frac{5103k}{18656} \mathbf{R}_v^5; \quad (26t)$$

$$\xi_{n(6)} = \frac{-g_1 - \sqrt{g_1^2 - 4g_2g_{0,4,n(6)}}}{2g_2}, \quad \omega^{n(6)} = \xi_{n(6)} + \kappa; \quad (26u)$$

$$\mathbf{R}_u^6 = v(\mathbf{u}^{n(6)}, \mathbf{v}^{n(6)})k, \quad \mathbf{R}_v^6 = v(\mathbf{u}^{n(6)}, \mathbf{v}^{n(6)})k; \quad (26v)$$

$$\mathbf{u}^{n(7)} = \mathbf{u}^n + \frac{9017k}{3168} \mathbf{R}_u^1 + \frac{500k}{1113} \mathbf{R}_u^3 + \frac{125k}{192} \mathbf{R}_u^4 - \frac{2187k}{6784} \mathbf{R}_u^5 + \frac{11k}{84} \mathbf{R}_u^6, \quad f_b^{n(7)} = K - \mathbf{u}_1^{n(7)}; \quad (26w)$$

$$\mathbf{v}_1^{n(7)} = -f_b^{n(7)}, \quad \mathbf{v}^{n(7)} = \mathbf{v}^n + \frac{9017k}{3168} \mathbf{R}_v^1 + \frac{500k}{1113} \mathbf{R}_v^3 + \frac{125k}{192} \mathbf{R}_v^4 - \frac{2187k}{6784} \mathbf{R}_v^5 + \frac{11k}{84} \mathbf{R}_v^6, \quad (26x)$$

$$\xi_{n(7)} = \frac{-g_1 - \sqrt{g_1^2 - 4g_2g_{0,4,n(7)}}}{2g_2}, \quad \omega^{n(7)} = \xi_{(7)} + \kappa; \quad (26y)$$

$$\mathbf{R}_u^7 = v(\mathbf{u}^{n(7)}, \mathbf{v}^{n(7)})k, \quad \mathbf{R}_v^7 = v(\mathbf{u}^{n(7)}, \mathbf{v}^{n(7)})k. \quad (26z)$$

The approximation with fifth-order Runge Kutta method given as

$$\mathbf{u}^{n+1} = \mathbf{u}^{n(7)}, \quad f_b^{n+1} = f_b^{n(7)}, \quad \mathbf{v}^{n+1} = \mathbf{v}^{n(7)}, \quad \xi_{n+1} = \xi_{n(7)}, \quad \omega^{n+1} = \omega^{n(7)}. \quad (27a)$$

represents the numerical solutions while the fourth-order Runge Kutta method given as

$$\tilde{\mathbf{u}}^{n+1} = \mathbf{u}^n + \frac{5179k}{57600} \mathbf{R}_u^1 + \frac{7571k}{16695} \mathbf{R}_u^3 + \frac{393k}{640} \mathbf{R}_u^4 - \frac{92097k}{339200} \mathbf{R}_u^5 + \frac{187k}{2100} \mathbf{R}_u^6 + \frac{k}{40} \mathbf{R}_u^7, \quad (27b)$$

$$\tilde{\mathbf{v}}^{n+1} = \mathbf{v}^n + \frac{5179k}{57600} \mathbf{R}_v^1 + \frac{7571k}{16695} \mathbf{R}_v^3 + \frac{393k}{640} \mathbf{R}_v^4 - \frac{92097k}{339200} \mathbf{R}_v^5 + \frac{187k}{2100} \mathbf{R}_v^6 + \frac{k}{40} \mathbf{R}_v^7, \quad (27c)$$

is used for the error estimation. A predefined tolerance ε is established such that the newly updated time step is computed based on the following condition (William and Saul, 1992)

$$k_{new} = \begin{cases} \eta k_{old} [\varepsilon / \max(e_u, e_v)]^{0.25}, & \max(e_u, e_v) < \varepsilon, \\ \eta k_{old} [\varepsilon / \max(e_u, e_v)]^{0.2}, & \max(e_u, e_v) \geq \varepsilon, \end{cases} \quad (28)$$

$\eta < 1$ and $\eta \approx 1$. Here, we choose $\eta = 0.9$. The new time step and solutions \mathbf{u}^{n+1} and \mathbf{v}^{n+1} are accepted as the optimal time step and numerical solutions if $\max(e_u, e_v) < \varepsilon$. Else, we recompute our solutions with a smaller time step till the condition $\max(e_u, e_v) < \varepsilon$ is satisfied.

4. Numerical Results

Example 1. Non-Dividend-Paying Options

We first consider non-dividend-paying options from the existing literature (Kim et al., 2013) with the following parameters

$$K = 100, \quad r = 5\%, \quad D = 0, \quad \sigma = 20\%. \quad (29)$$

We chose the interval of $x \in [0,3]$. The focus in this example is to compute the convergence rate of our numerical method and verify that it is consistent with the theoretical convergence rate. Here, we computed the convergence rate with the fourth-order Runge-Kutta method, a constant time step of $k = 10^{-6}$ and varying step sizes $h = 0.1, 0.05, 0.025,$ and 0.0125 . The results were displayed in Table 1. From

Table 1, we observed that the numerical convergence rate is in good agreement with the theoretical convergence rate.

Table 1. Errors and convergence rate in space with a third-order Robin boundary ($k = 10^{-6}, T = 0.25$).

h	Asset option		Delta option	
	maximum error	convergence rate	maximum error	convergence rate
0.1	~	~	~	~
0.05	9.105×10^{-1}	~	5.972×10^0	~
0.025	3.232×10^{-2}	4.777	3.290×10^{-1}	4.182
0.0125	2.075×10^{-3}	4.001	2.865×10^{-2}	3.521
Optimal exercise boundary				
	values	maximum error	convergence rate	
0.1	87.744120699565300	~		
0.05	86.833647682786200	9.105×10^{-1}	~	
0.025	86.803304297354500	3.034×10^{-2}	4.907	
0.0125	86.805290298684800	1.986×10^{-3}	3.933	

Even though implementation of the classical fourth-order time integration method could improve the accuracy of our numerical solution substantially, it could be tempting to assume that it is the reason why the fourth-order numerical convergence rate in space was recovered in our present method. We would rather love to point out that the recovery of the fourth-order convergence rate in space is due to our improvement and derivation in (13) and (14). To validate this claim, we implement the Crank-Nicholson scheme without further improvement in terms of strategic Rannacher time-stepping, mesh refinement, and smoothing of initial conditions. To this end, we first obtain an approximation of the optimal exercise boundary from the Crank-Nicholson scheme as follows:

$$f_b^n + \frac{k}{2} \frac{\partial f_b^n}{\partial \tau} = f_b^{n+1} - \frac{k}{2} \frac{\partial f_b^{n+1}}{\partial \tau}. \quad (30a)$$

Because the optimal exercise boundary is computed from the analytical approximation for the Crank-Nicholson scheme, we use the third-order analytical approximation as follows:

$$\frac{\partial f_b^n}{\partial \tau} = \left(\frac{-m_1^2 - \sqrt{m_2 - 4m_2 m_{0,3,n}}}{2g_0} \right) f_b^n(\tau) = \varpi^n f_b^n, \quad (30b)$$

$$f_b^n \left(1 + \frac{k}{2} \varpi^n \right) = f_b^{n+1} \left(1 - \frac{k}{2} \varpi^{n+1} \right), \quad f_b^{n+1} = \frac{\left(1 + \frac{k}{2} \varpi^n \right)}{\left(1 - \frac{k}{2} \varpi^{n+1} \right)} f_b^n. \quad (30c)$$

$$m_2 = \frac{2L'(0, \tau) \gamma_2 \tilde{x}^3}{3\sigma^4}, \quad (30d)$$

$$m_1 = \left[\frac{4L'(0, \tau)\kappa}{3\sigma^4} - \frac{2Df_b(\tau)}{3\sigma^2 L'(0, \tau)} \right] \gamma_2 \tilde{x}^3 - \frac{2L'(0, \tau)\gamma_1 \tilde{x}^2}{3\sigma^2}, \quad (30e)$$

$$m_{0,3} = \left[\frac{2L'(0, \tau)\kappa^2}{3\sigma^4} + \frac{Df_b(\tau)\kappa}{6\sigma^4 L'(0, \tau)} - \frac{(Df_b(\tau))^2}{12\sigma^4 [L'(0, \tau)]^3} + \frac{rL'(0, \tau)}{2\sigma^2} - \frac{Df_b(\tau)}{4\sigma^2 L'(0, \tau)} \right] \gamma_2 \tilde{x}^3 \\ - \left[\frac{2L'(0, \tau)}{3\sigma^2} \kappa + \frac{Df_b(\tau)}{3\sigma^2 L'(0, \tau)} \right] \gamma_1 \tilde{x}^2 + \gamma_0 \tilde{x} L'(0, \tau) - M_3(\tilde{x}, \tau), \quad (30f)$$

$$M_3(\tilde{x}, \tau) = \alpha_1 L(\tilde{x}, \tau) + \alpha_2 L(2\tilde{x}, \tau) + \alpha_3 L(3\tilde{x}, \tau). \quad (30g)$$

$$\alpha_1 = 81, \quad \alpha_2 = -\frac{81}{8}, \quad \alpha_3 = 1; \quad (30h)$$

$$\gamma_0 = \frac{255}{4}, \quad \gamma_1 = \frac{99}{4}, \quad \gamma_2 = \frac{9}{2}. \quad (30i)$$

From (23), we computed the left-hand boundary values of (3a) and (3b) and discretized the interior nodes in time with the Crank-Nicholson scheme. We then computed the convergence rate of the optimal exercise boundary, asset option, and option sensitivity which we listed in Table 2. From Table 2, one can easily observe that the convergence rate in space with the Crank-Nicholson discretization in time is in close agreement with the theoretical convergence rate. The major advantage of implementing 5(4) Runge-Kutta embedded pairs is to employ a fifth-order time integration method and allow optimal time step selection in each time level. The latter advantage could further be very useful in detecting unknown locations with large variations in a system due to discontinuity, oscillation, etc.

Table 2. Errors and convergence rate in space with third-order Robin boundary and Crank-Nicholson scheme. ($k = 10^{-6}, T = 0.5$).

h	Asset option		Delta option	
	maximum error	convergence rate	maximum error	convergence rate
0.1	~	~	~	~
0.05	7.452×10^{-1}	~	1.173×10^0	~
0.025	4.650×10^{-2}	4.002	2.363×10^{-1}	2.311
0.0125	3.300×10^{-3}	3.817	1.362×10^{-2}	4.117
0.00625	2.171×10^{-4}	3.926	8.179×10^{-4}	4.057
Optimal exercise boundary				
	values	maximum error	convergence rate	
0.1	84.6168895718962	~		
0.05	83.8717223863237	7.452×10^{-1}	~	
0.025	83.9162106246566	4.449×10^{-2}	4.002	
0.0125	83.9193524617783	3.142×10^{-3}	3.824	
0.00625	83.9195594221456	2.070×10^{-5}	3.924	

Example 2. Dividend-Paying Options

For the dividend-paying American options, we consider two examples from the work of Kim et al. (2013) and Tangman et al. (2008) with the following parameters:

$$K = 100, \quad T = 0.5, \quad r = 5\%, \quad D = 3\%, \quad \sigma = 20\%, \quad (31a)$$

$$K = 100, \quad T = 0.5, \quad r = 7\%, \quad D = 3\%, \quad \sigma = 40\%. \quad (31b)$$

It is well known that the performance and accuracy of the adaptive Runge-Kutta methods depend on the type of model under investigation. Not much has been done on implementing these embedded pairs in the option pricing problem. For our present model with a discontinuity at the left boundary and time-dependent coefficient, it will be ideal to extensively compare the existing 5(4) Runge-Kutta embedded pair to validate the one that performs optimally. The first objective in this example is to compare the performance of our present method with several 5(4) embedded pairs. The second objective is to compare our numerical results of the asset option, option sensitivity, and optimal exercise boundary with the existing methods. Furthermore, we compute and verify the convergence rates of the present method. To this end, we label the Runge-Kutta 5(4) pairs as follows:

- Dormand and Prince 5(4) embedded pair (RK-DR)
- Modified 5(4) Runge-Kutta-Fehlberg method based on Cash and Karp coefficients (RK-CK)
- Simon and Tsitorous 5(4) embedded pair (RK-ST)
- Bogacki and Shampine 5(4) embedded pair (RK-BS)
- Papakostas and Papageorgiou 5(4) embedded pair (RK-NEW)

With (24a), we compared the performance and accuracy of several well-known 5(4) Runge-Kutta pairs. These pairs are fifth-order accurate in time. We intentionally use a large tolerance ($\varepsilon = 10^{-3}$, $\varepsilon = 10^{-4}$, or $\varepsilon = 10^{-5}$) in most cases in this example. This is because we intend to investigate the performance of these embedded pairs with varying large tolerances and step sizes. We also compared the numerical results of the asset option from our present method with the method of Wu and Kwok (1997), Kim et al. (2013), and Muthuraman (27) which we label as WK, KIM, and MBM, respectively. We chose the method of Cox et al. (1979) as the benchmark result. Furthermore, we used a very small step size to compute the optimal exercise boundary. Using the former as a benchmark, we then compared the results of the optimal exercise boundary obtained with these pairs when ε and h were varied. We also compared the total CPU time required to obtain the numerical results of the optimal exercise boundary with these pairs. The results were listed in Tables 3-5 and displayed in Fig. 1.

With a tolerance of $\varepsilon = 10^{-5}$, we observed from Table 3 that we have a more accurate numerical solution when $h = 0.025$ with RK-DP and RK-BS. Furthermore, with $h = 0.01$ and 10^{-4} , the optimal exercise boundary obtained with RK-DP and RK-BS is very close to the benchmark result and requires less total CPU time and average time step when compared to RK-ST and RK-CK. Hence RK-DP and RK-BS present more superior advantages in terms of accuracy and computational cost. It is worth mentioning that we obtained numerical divergence with RK-NEW.

With (24b), we used very large step sizes to compute the delta option and compared the result with the methods of Brennan and Schwartz (1977), Han and Wu (2003), Ikonen and Toivanen (2004), and Forsyth and Vetzal (2002) which we label as BS, HW, OS, and PENALTY, respectively. The Binomial method of Leisen and Reimer (1996) is used as the benchmark result. The results were listed in Table 6.

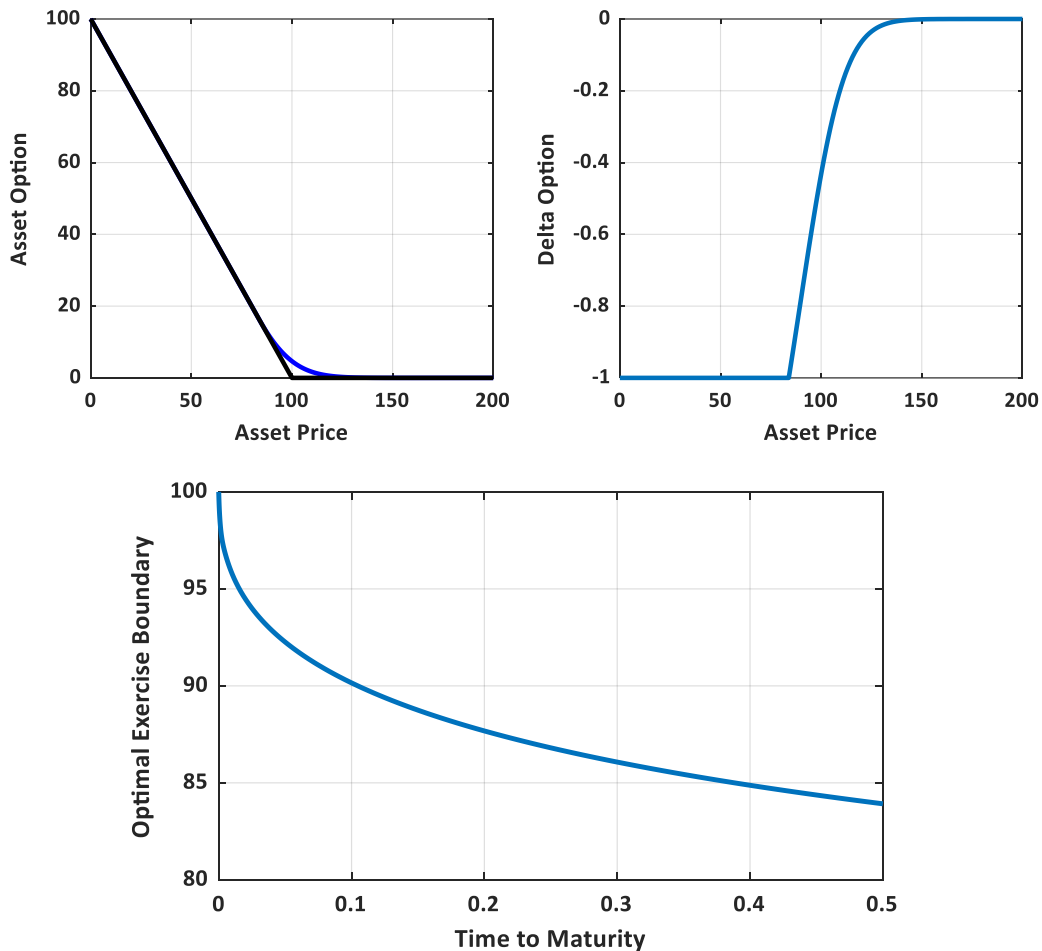


Fig. 1a. Plots of the option values and optimal exercise boundary in (24a) without dividend ($\tau = T$).

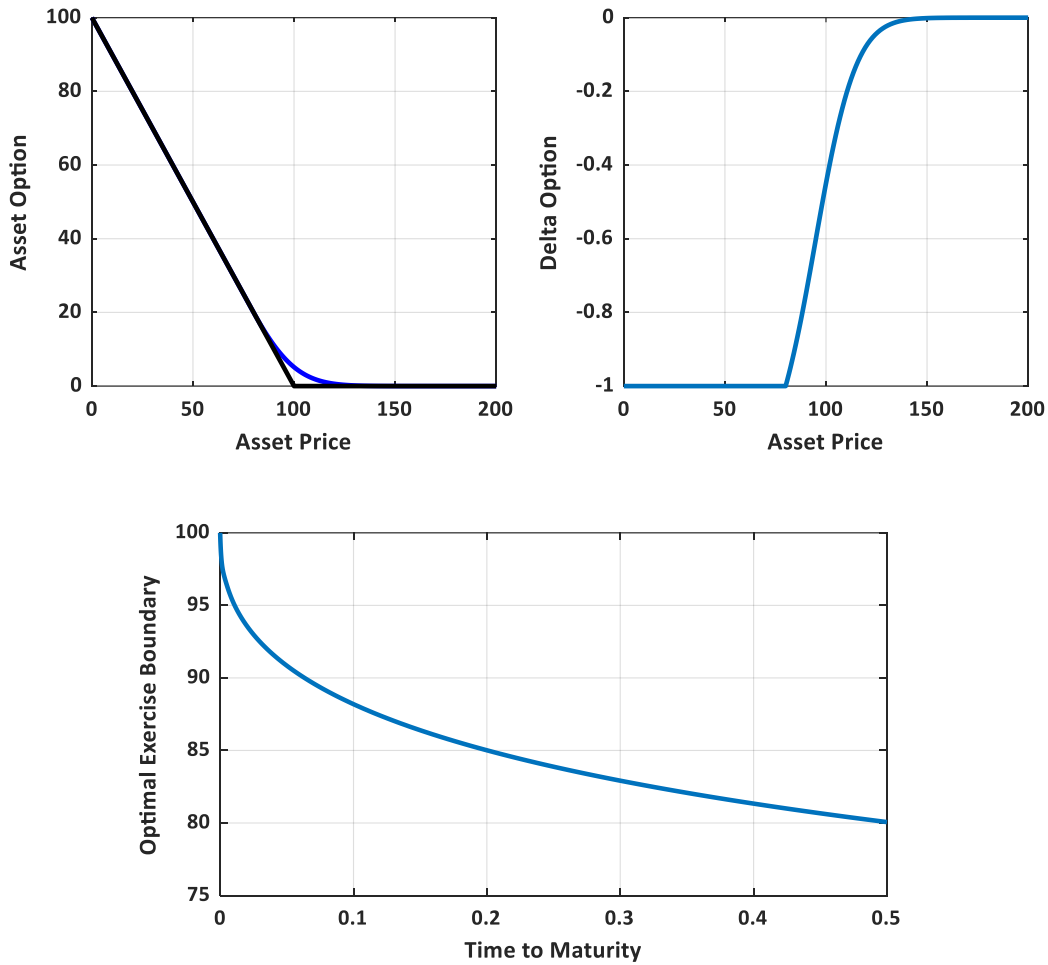


Fig. 1b. Plots of the option values and optimal exercise boundary in (24a) with dividend ($\tau = T$).

With $h = 0.075$ and $\varepsilon = 10^{-5}$, the results we obtained from our pairs are very close to the benchmark results. This is an indication of the superiority of our approach in terms of achieving accuracy with very coarse grids. In terms of total CPU time in seconds, RK-DP and RK-BS are superior to RK-CK AND RK-ST. We also plotted the time step against the time level and displayed the result in Fig. 2. The common characteristic in the plots is that a very small time step is required very close to the free boundary. This is because of the piecewise nature of the asset option and the discontinuity in the delta option at the payoff. Hence small time would be required in that region. This is a well-known behavior of RK-embedded pairs. In Fig. 2, the horizontal red line represents the average optimal time step. We further observed that this value is smaller in RK-DP and RK-BS when compared with RK-ST and RK-CK.

Table 3. Comparison of the asset option with (24a) and the embedded 5(4) RK pairs ($\varepsilon = 10^{-5}, k = h$).

S	True Value	WK			MBM		KIM	
80	20.0000	20.0000			20.0000		20.0000	
90	11.1551	11.1513			11.1526		11.1544	
100	5.1496	5.1435			5.1444		5.1496	
110	1.9491	1.9461			1.9455		1.9509	
120	0.6132	0.6113			0.6155		0.6153	
		RK-DP			RK-CK			
	$h = 0.025$	0.0125	0.01	0.025	0.0125	0.01		
80	20.0000	20.0000	20.0000	20.0000	20.0000	20.0000	20.0000	
90	11.1550	11.1548	11.1548	11.1550	11.1550	11.1547	11.1547	
100	5.1494	5.1494	5.1494	5.1489	5.1489	5.1489	5.1490	
110	1.9487	1.9487	1.9488	1.9477	1.9480	1.9481	1.9481	
120	0.6130	0.6130	0.6131	0.6121	0.6124	0.6125	0.6125	
		RK-ST			RK-BS		RK-NEW	
	$h = 0.025$	0.0125	0.01	0.025	0.0125	0.01	0.0125	0.01
80	20.0000	20.0000	20.0000	20.0000	20.0000	20.0000	diverge	diverge
90	10.1550	10.1547	10.1547	10.1550	10.1548	10.1548	diverge	diverge
100	5.1488	5.1489	5.1490	5.1494	5.1494	5.1494	diverge	diverge
110	1.9474	1.9479	1.9481	1.9487	1.9487	1.9488	diverge	diverge
120	0.6118	0.6123	0.6125	0.6130	0.6130	0.6131	diverge	diverge

Table 4. Values of the optimal exercise boundary with RK-DP and very small step sizes.

h	0.01	0.005	0.0025
$f_b(\tau)$	80.06279138725	80.06250056775	80.06233787425

Table 5a. Performance of the embedded pairs on fixed step size ($h = 0.01, k = h$) and varying tolerance.

	RK-DP			RK-CK		
ε	10^{-3}	10^{-4}	10^{-5}	10^{-3}	10^{-4}	10^{-5}
Total CPU time(s)	11.81	12.33	13.38	23.73	64.31	187.79
$f_b(\tau)$	80.0621	83.0628	83.0628	80.0674	80.0637	80.0631
Min. optimal time step	2.72e-5	7.57e-6	2.25e-6	4.06e-6	1.26e-6	3.95e-7
Ave. optimal time step	1.85e-3	1.79e-3	1.69e-3	7.86e-4	2.77e-4	8.99e-5
Max. optimal time step	2.62e-3	2.13e-3	2.14e-3	2.19e-3	7.82e-4	2.64e-4
	RK-ST			RK-BS		
ε	10^{-3}	10^{-4}	10^{-5}	10^{-3}	10^{-4}	10^{-5}
Total CPU time(s)	12.92	20.01	38.24	17.84	18.57	19.48
$f_b(\tau)$	80.0681	80.0645	80.0630	80.0658	80.0628	80.0628
Min. optimal time step	3.45e-5	6.95e-6	4.88e-6	7.78e-5	2.41e-5	7.23e-6
Ave. optimal time step	1.61e-3	9.73e-4	5.29e-4	2.36e-3	2.31e-3	2.30e-3
Max. optimal time step	2.21e-2	6.84e-3	1.43e-3	4.42e-3	5.46e-2	7.37e-3

Table 5b. Performance of the embedded pairs on fixed tolerance and varying step size ($\varepsilon = 10^{-5}, k = h$).

	RK-DP			RK-CK		
h	0.025	0.0125	0.01	0.025	0.0125	0.01
Total CPU time(s)	1.21	6.15	13.38	27.13	105.25	187.79
$f_b(\tau)$	80.0611	80.0628	80.0628	80.0604	80.0629	80.0631
Min. optimal time step	1.93e-5	3.79e-6	2.25e-6	2.54e-6	6.58e-7	3.95e-7
Ave. optimal time step	6.41e-3	2.45e-3	1.69e-3	1.59e-4	1.04e-5	8.99e-5
Max. optimal time step	1.25e-2	3.36e-3	2.14e-3	6.23e-4	3.29e-4	2.64e-4
	RK-ST			RK-BS		
h	0.025	0.0125	0.01	0.025	0.0125	0.01
Total CPU time(s)	5.03	20.36	38.24	1.22	7.89	19.48
$f_b(\tau)$	80.0603	80.0628	80.0630	80.0611	80.0629	80.0628
Min. optimal time step	4.41e-5	8.08e-6	4.88e-6	6.23e-8	1.22e-5	7.23e-6
Ave. optimal time step	1.00e-3	6.36e-4	5.29e-4	9.43e-3	3.40e-3	2.30e-3
Max. optimal time step	4.22e-3	2.00e-3	1.43e-3	3.07e-2	1.10e-2	7.37e-3

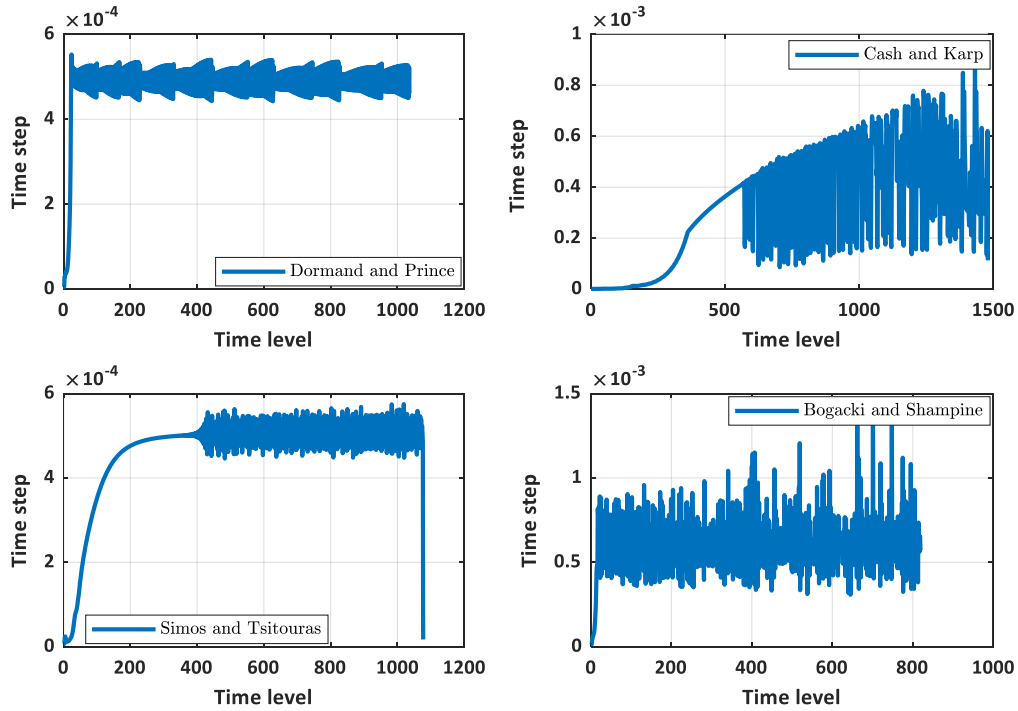


Fig. 2a. Optimal time step in each time level with $\varepsilon = 10^{-3}, h = 0.01$ and $k = h$.

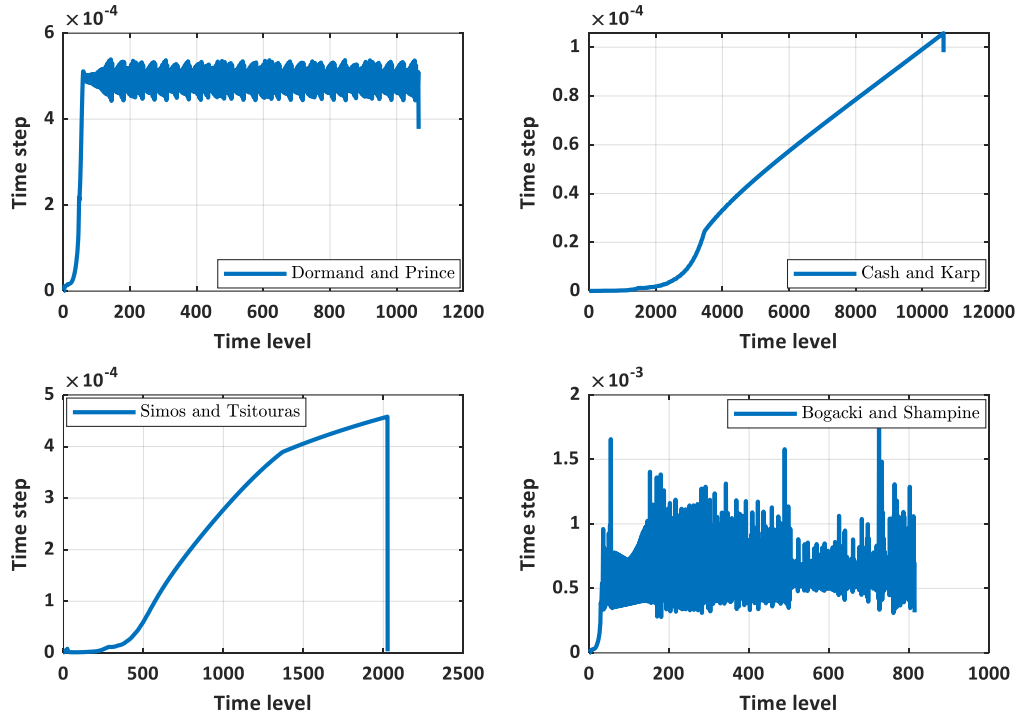


Fig. 2b. Optimal time step in each time level with $\varepsilon = 10^{-5}$, $h = 0.01$ and $k = h$.

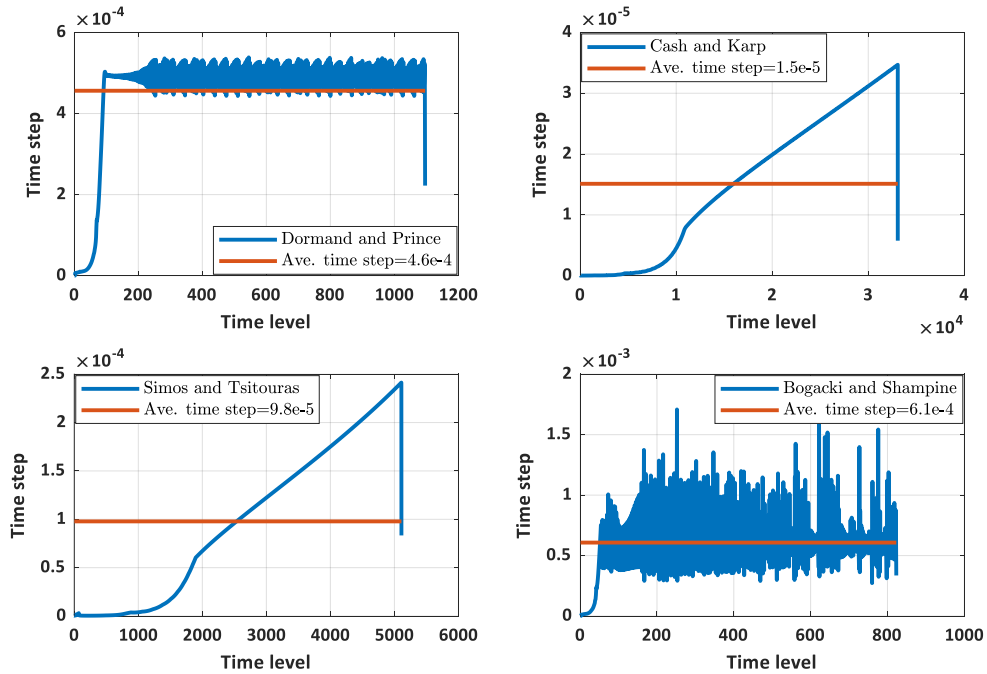


Fig. 2c. Optimal time step in each time level and average time step with $\varepsilon = 10^{-6}$, $h = 0.01$ and $k = h$.

Table 6. Comparison of the delta option with (24b) and the embedded 4(5) RK pairs ($\varepsilon = 10^{-5}$, $k = h$).

S	True Value	BS2	HW	OS	PENALTY	
80	-0.7501	-0.7501	-0.7489	-0.7501	-0.7502	
90	-0.5791	-0.5791	-0.5791	-0.5791	-0.5791	
100	-0.4229	-0.4229	-0.4222	-0.4230	-0.4229	
110	-0.2943	-0.2943	-0.2938	-0.2943	-0.2943	
120	-0.1968	-0.1968	-0.1965	-0.1968	-0.1968	
		RK-DP			RK-CK	
	$h = 0.075$	0.05	0.03	0.075	0.05	0.03
80	-0.7500	-0.7501	-0.7501	-0.7501	-0.7501	-0.7502
90	-0.5792	-0.5791	-0.5791	-0.5793	-0.5792	-0.5791
100	-0.4231	-0.4230	-0.4229	-0.4231	-0.4230	-0.4229
110	-0.2944	-0.2943	-0.2943	-0.2944	-0.2943	-0.2943
120	-0.1968	-0.1968	-0.1968	-0.1968	-0.1968	-0.1968
Total CPU time(s)	0.50	0.79	1.28	6.26	9.67	22.25
		RK-ST			RK-BS	
	$h = 0.075$	0.05	0.03	0.075	0.05	0.03
80	-0.7502	-0.7502	-0.7502	-0.7500	-0.7501	-0.7502
90	-0.5792	-0.5792	-0.5792	-0.5793	-0.5791	-0.5791
100	-0.4230	-0.4230	-0.4230	-0.4231	-0.4230	-0.4229
110	-0.2943	-0.2943	-0.2943	-0.2944	-0.2943	-0.2943
120	-0.1968	-0.1968	-0.1968	-0.1968	-0.1968	-0.1968
Total CPU time(s)	1.12	2.37	5.45	0.59	0.76	1.88

5. Conclusion

We have proposed an efficient and high-order numerical method for pricing free boundary non-dividend and dividend-paying options. The major challenge in solving the free boundary option pricing model is to recover the high order convergence rate. It has been shown in previous literature that even with an efficient fourth-order numerical scheme, only second-order convergence can be expected. To recover the high order convergence rate from our present method, we derive a high order analytical approximation from the left boundary and obtained a precise value of the time-dependent coefficient that introduces nonlinearity in the model. Furthermore, we introduce a special boundary treatment that enables us to compute the optimal exercise boundary without further discretization in time. With the implementation of a compact finite difference scheme, we then carried further investigation on the performance of our present method with several 5(4) RK-embedded pairs. This is by no means an exhaustive investigation; however, it gives us an insight into how some of these pairs can significantly improve both the accuracy and computational cost of our numerical solutions. One of the reasons for this investigation is because some of these pairs are model-dependent. From the numerical experiment, we observe that RK-DP and

RK-BS perform significantly better than RK-TS and RK-CK. Moreover, we achieve numerical divergence with RK-NEW. We compute the convergence rate in space of our present method and validate that the numerical convergence rate is in good agreement with the theoretical convergence rate. By further comparing with other existing methods using the example in (24a) and (24b), we confirm that our present method provides more accurate numerical solutions with very coarse grids.

Funding

No funding was received from any resource.

Availability of Data and Material (Data Transparency)

The data could be shared at a reasonable request.

Conflict of interest

The author declares that he has no conflict of interest.

Reference

1. Ballestra, L. V. (2018). Fast and accurate calculation of American option prices. *Decisions in Economics and Finance*, 41, 399-426. <https://doi.org/10.1007/s10203-018-0224-1>
2. Bhatt, H. P., & Khaliq, A. Q. M. (2016). Fourth-order compact schemes for the numerical simulation of coupled Burgers' equation. *Computer Physics Communications*, 200, 117-138. <https://doi.org/10.1016/j.cpc.2015.11.007>
3. Bogacki, P. (1996). A family of Parallel Runge-Kutta Pairs. *Computers Math. Applic.*, 31, 23-31.
4. Bogacki, P., & Shampine, L. F. (1996). An efficient Runge-Kutta (4,5) pair. *Computers Math. Applic.*, 32, 15-28.
5. Brennan M., & Schwartz, E. (1997). The valuation of American put options, *J. Fin.*, 32, 449–462.
6. Cash, R. J., & Karp, A. H. (1990). A variable order Runge-Kutta for initial value problems with rapidly varying right-hand sides. *ACM Transaction on Mathematical Software*, 16, 201-222.
7. Cen, Z. & Chen, W. (2019). A HODIE finite difference scheme for pricing American options. *Advances in Difference Equations* 67.
8. Chen, X., & Chan, J. (2006). A Mathematical Analysis of the Optimal Exercise Boundary American Put Options. *SIAM Journal on Mathematical Analysis*, 38, 1613-1641.

9. Christara, C. C., & Dang, D. M. (2011). Adaptive and high-order methods for valuing American options. *Journal of Computational Finance*, 14, 73-113.
10. Company, R., Egorova, V.N., & Jódar, L. (2016). A positive, stable, and consistent front-fixing numerical scheme for American options. In: Russo G., Capasso V., Nicosia G., Romano V. (eds) *Progress in Industrial Mathematics at ECMI 2014. Mathematics in Industry*, 22, 57-64.
11. Company, R., Egorova, V.N., & Jódar, L. (2014). Solving American option pricing models by the front fixing method: numerical analysis and computing. *Abstract and Applied Analysis*, 2014, 146745.
12. Cox, J. C., Ross, S. A., & Rubinstein, M. (1979). Option pricing: a simplified approach. *Journal of Financial Economics*, 7, 229–263.
13. Dormand, J. R., & Prince, J. P. (1980). A family of embedded Rung-Kutta formulae. *Journal of Computational and Applied Mathematics*, 6, 19-26
14. Egorova, V. N., Company, R., & Jódar, L. (2016). A new efficient numerical method for solving American option under regime switching model. *Computers and Mathematics with Applications*, 71, 224–237.
15. Fehlberg, E. (1969). Low-order classical Runge-Kutta formulas with step size control and their application to some heat transfer problems. NASA Technical Report 315.
16. Forsyth, P. A., & Vetzal, K. R. (2002). Quadratic convergence of a penalty method for valuing American options. *SIAM J. Sci. Comput.*, 23, 2096–2123.
17. Goodman, J., & Ostrov, D. N. (2002). On the early exercise boundary of the American put option. *SIAM Journal of Applied Mathematics*, 62, 1823-1835.
18. Hajipour, M. & Malek, A. (2015). Efficient high-order numerical methods for pricing option. *Computational Economics*, 45, 31-47.
19. Han, H. & Wu, X. (2003). A fast numerical method for the Black-Scholes equation for American options. *SIAM Journal of Numerical Analysis*, 41, 2081-2095.
20. Holmes, A. D., & Yang, H. (2008). A front-fixing finite element method for the valuation of American options. *SIAM Journal of Scientific Computing*, 30, 2158-2180.
21. Hoover W. G., Sprot, J. C., & Hoover C. G. (2016). Adaptive Runge-Kutta integration for stiff systems: Comparing Nose and Nose-Hoovers dynamics for the harmonic oscillator. *American Journal of Physics*, 84, 786.
22. Ikonen, S., & Toivanen, J. (2004). Operator splitting methods for American option pricing, *Appl. Math. Lett.*, 17, 809–814.

23. Ketcheson, D. I., Mortenson, M., Parsani, M., & Schilling, N. (2020). More efficient time integration for Fourier pseudospectral DNS of incompressible turbulence. *Int. J. Numer. Meth. Fluids*, 92, 79–93.
24. Kim, B. J., Ma, Y., & Choe, H. J. (2013). A simple numerical method for pricing an American put option. *Journal of Applied Mathematics*, 2013, 128025.
25. Kim, B. J., Ma, Y., & Choe, H. J. (2017). Optimal exercise boundary via intermediate function with jump risk. *Japan Journal of Industrial and Applied Mathematics*, 34, 779-792.
26. Leisen, D., & Reimer M. (1996). Binomial models for option valuation—examining and improving convergence, *Appl. Math. Fin.*, 3, 319–346.
27. Macdougall, T., & Verner, J. H. (2002). Global error estimators for 7, 8 Runge-Kutta pairs. *Numerical Algorithm*, 31, 215-231.
28. Mallier, R. (2002). Evaluating approximations to the optimal exercise boundary for American options. *Journal of Applied Mathematics* 2, 71–92.
29. Muthuraman, K. (2008). A moving boundary approach to American option pricing. *Journal of Economics, Dynamics, and Control*, 32, 3520–3537.
30. Nielsen, B. F., Skavhaug O., & Tveito, A. (2002). A penalty and front-fixing methods for the numerical solution of American option problems. *Journal of Computational Finance*, 5, 69-97.
31. Oosterlee, C. W. Leentvaar, C. C. W. & Huang, X. (2005). Accurate American option pricing by grid stretching and high order finite differences. Working Papers, DIAM, Delft University of Technology, Delft, The Netherlands.
32. Papakostas S.N., & Papageorgiou, G. (1996). A family of fifth-order Runge-Kutta pairs. *Mathematics of Computation*, 65, 1165-1181.
33. Pooley, D. M., Vetzal, K. R., & Forsyth, P. A. (2003). Convergence remedies for non-smooth payoffs in option pricing. *Journal of Computational Finance*, 6(4), 25-40. Doi: 10.21314/JCF.2003.101
34. Simos, T. E. (1993). A Runge-Kutta Fehlberg method with phase-lag of order infinity for initial-value problems with oscillation solution. *Computers and Mathematics with Application*, 25, 95-101.
35. Simos, T. E., & Papakaliatakis, G. (1998). Modified Runge-Kutta Verner methods for the numerical solution of initial and boundary-value problems with engineering application. *Applied Mathematical Modelling*, 22, 657-670.
36. Simos, T. E., & Tsitouras, C. (2018). Fitted modifications of classical Runge-Kutta pairs of orders 5(4). *Math Meth Appl Sci.*, 41, 4549–4559.

37. Song, H., Zhang, K., & Li, Y. (2017). Finite element and discontinuous Galerkin methods with perfect matched layers for American options. *Numerical Mathematics Theory Methods and Application*, 10, 829-521.
38. Tangman, D. Y. Gopaul, A., & Bhuruth, M. (2008). A fast high-order finite difference algorithm for pricing American options. *Journal of Computational and Applied Mathematics*, 222, 17-29 (2008)
39. Tsitouras, C. (1998). A parameter study of explicit Runge-Kutta pairs of orders 6(5). *Applied Mathematics Letter*, 11, 65-69.
40. Wilkie, J., & Cetinbas, M. (2005). Variable-stepsize Runge-Kutta for stochastic Schrodinger equations. *Physics Letters A*, 337, 166-182.
41. William, H. P., & Saul, A. T. (1992). Adaptive stepsize Runge-Kutta Integration. *Computer in Physics*, 6, 188.
42. Wu, L., & Kwok, Y.K. (1997). A front-fixing method for the valuation of American options. *J. Finance. Eng.*, 6, 83–97.
43. Yan, Y., Dai, W., Wu, L., & Zhai, S. (2019). Accurate gradient preserved method for solving heat conduction equations in double layers. *Applied Mathematics and Computation*, 354, 58-85.
44. Zhang, K., Song, H., & Li, J. (2014). Front-fixing FEMs for the pricing of American options based on a PML technique. *Applicable Analysis: An International Journal*, 94, 1-29.
45. Zhao, J. (2007). Highly accurate compact mixed method for two point boundary value problem. *Applied Mathematics and Computation*, 188, 1402-1418.
46. Zhao, J., Davidson, M., & Corless, R. M. (2007). Compact finite difference method for American option pricing. *Journal of Computational and Applied Mathematics*, 206, 306-321.